

New Fluorescent Dyes in the Red Region for Biodiagnostics

M. Sauer,^{1,3} K.-T. Han,¹ R. Müller,¹ S. Nord,¹ A. Schulz,¹ S. Seeger,¹ J. Wolfrum,¹
J. Arden-Jacob,² G. Deltau,² N. J. Marx,² C. Zander,² and K. H. Drexhage²

Received July 29, 1994; revised December 14, 1994; accepted December 16, 1994

The increased sensitivity together with the advent of low-cost optical sources and detectors in the visible-near IR region has led us to current efforts to develop new efficient fluorescent labels for biodiagnostics with absorption and emission beyond 600 nm. In view of the general fluorescence decrease with increasing emission wavelength, we investigated the possibility to shift the absorption of rhodamine dyes toward the region 620–670 nm. The hydrophobic nature of all known long-wavelength dyes results in the tendency to form intra- and intermolecular aggregates in hydrophilic solvents, especially in aqueous environment. Due to the aggregation with biological materials, fluorescence quenching of the dyes is often observed. New strategies for prevention of these processes are considered.

KEY WORDS: Fluorescence; photochemistry; rhodamine dyes; time-resolved spectroscopy.

INTRODUCTION

The importance of fluorescent dyes for qualitative and quantitative determination of analytes has increased considerably in recent years.^(1–5) Using fluorescent dyes, an extremely high sensitivity can be achieved. Furthermore, time- and position-resolved detection without contacting the analyte is possible. Typically the fluorescent probes or markers are identified and quantitated by their absorption and fluorescence emission wavelengths and intensities. The sensitivity achievable with a fluorescent label is directly proportional to the molar extinction coefficient for absorption and the quantum yield of fluorescence. The extinction coefficient typically has maximum values of about $10^5 \text{ L mol}^{-1} \text{ cm}^{-1}$ in organic dyes and the quantum yield may approach values close to 100%. Absorption and emission spectra as well as the

fluorescence quantum yield and lifetime are dependent on environmental factors. For labeling of biological compounds, e.g., antibodies or DNA bases, the fluorescent dye must carry a functional group suitable for a mild covalent binding reaction, preferably with free amino groups of the analyte. Furthermore, the dye should be as hydrophilic as possible to avoid aggregation and nonspecific binding in aqueous environment.

Since the introduction of fluorescein isocyanate for immunofluorescence by Coons *et al.*,⁽⁶⁾ it has been the fluorochrome of choice in many applications. This label exhibits a high fluorescence quantum yield, although the Stokes shift is rather small. Furthermore, this dye is quite hydrophilic. Therefore it shows only little nonspecific affinity to biological material. More recently the isocyanate as the active intermediate for covalent coupling to analytes has been replaced by isothiocyanate as a more convenient and safe derivative.⁽⁷⁾ Rhodamine dyes are often used as alternatives to fluorescein. Owing to their structural rigidity, rhodamines show high fluorescence quantum yields. Like fluorescein dyes, rhodamines also exhibit a small Stokes shift of about 20–30 nm (Fig. 1). They are applied as complementary probes together

¹ Physikalisch-Chemisches Institut, Universität Heidelberg, 69120 Heidelberg, Germany.

² Institut für Physikalische Chemie, Universität-Gesamthochschule Siegen, 57068 Siegen, Germany.

³ To whom correspondence should be addressed.

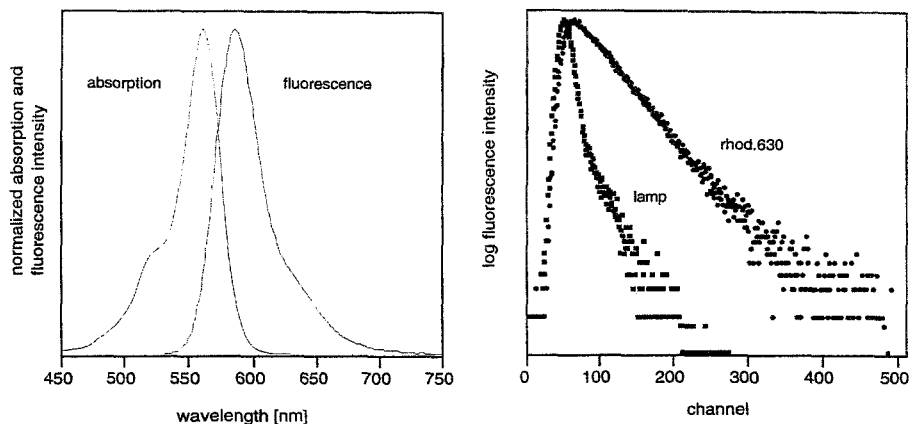


Fig. 1. Normalized absorption and emission spectrum of rhodamine 630 in ethanol (left). Fluorescence decay of rhodamine 630 in ethanol and lamp profile (512 channels, 100 ps/channel) measured with a hydrogen-filled flashlamp using a time-correlated single-photon counting technique (right).

with fluorescein in double-label staining, as energy acceptors in fluorescence energy transfer immunoassays, and as fluorescent markers in DNA sequencing. Rhodamine dyes are in general far more stable than fluorescein.⁽⁴⁾

The π -electron distribution in the chromophore of rhodamine dyes can be described approximately by two identical mesomeric structures, in which the positive charge is located on either of the two nitrogen atoms (Fig. 2). Thus in these dyes there is no permanent electric dipole moment parallel to the long axis of the molecule in either the ground or the excited state. The transition moment of the main long-wavelength absorption band is oriented parallel to the long axis of the molecule. The absorption spectrum is determined by this symmetrical π -electron system extending across the diaminoxanthene frame. Because the dipole moment does not change upon excitation, the absorption maximum shows only little dependence on the polarity of the solvent. On deprotonation of the carboxyl group (rhodamine B, rhodamine 101) a hypsochromic shift of about 10 nm occurs.⁽⁸⁾ The esterified derivatives such as rhodamine 630 and rhodamine 6G do not exhibit a pH-dependent absorption or emission spectrum.

The fluorescence efficiency of rhodamines shows a peculiar dependence on the substitution pattern of the amino groups. If the amino groups are fully alkylated, e.g., in the case of rhodamine B, the fluorescence efficiency is strongly dependent on solvent viscosity and temperature. These effects can be attributed to some kind of mobility of the diethylamino groups in the excited state, which is enhanced with increasing temperature and reduced with increasing viscosity. However, the de-

crease in lifetime by changing from ethanol to water, a solvent with nearly the same viscosity, demonstrates that also other solvent properties such as solvent polarity influence the excited-state lifetime and thereby the fluorescence efficiency (Table I). On the other hand, if the amino groups are only partially alkylated or incorporated in rigid six-membered rings, e.g., in the case of rhodamine 6G, rhodamine 101, and rhodamine 630, the fluorescence efficiency is close to unity and nearly independent of solvent polarity and temperature (Table I).⁽⁸⁻¹⁰⁾

Although rhodamine B and rhodamine 101 carry an unesterified carboxyl group, this group is not amenable to covalent coupling to analytes, due to steric hindrance. Because the amino groups are rigidized by a single six-membered ring, a dye such as rhodamine 630 offers the possibility to attach at the amino groups a functional group for covalent coupling to the analytes. Since the carboxyphenyl substituent is held in a position nearly perpendicular to the xanthene moiety, it is not part of the chromophoric system. Hence it has only a minor influence on the absorption and emission spectrum of the dye. However, the fluorescence lifetime is increased by about 300 ps compared to the dye without the carboxyphenyl substituent (compare rhodamine 630 and pyronin 630, Table I and Fig. 2).

Removal of the bulky *o*-carboxyl group leads to so-called rosamines, which show reduced quantum efficiency in fluid solvents such as ethanol, methanol, or water.⁽¹¹⁾ In rosamine 1 (Fig. 2) the steric hindrance for torsion of the phenyl group is reduced, leading to a configuration in which the planes of the phenyl substituent and the xanthene ring system nearly approach coplanar-

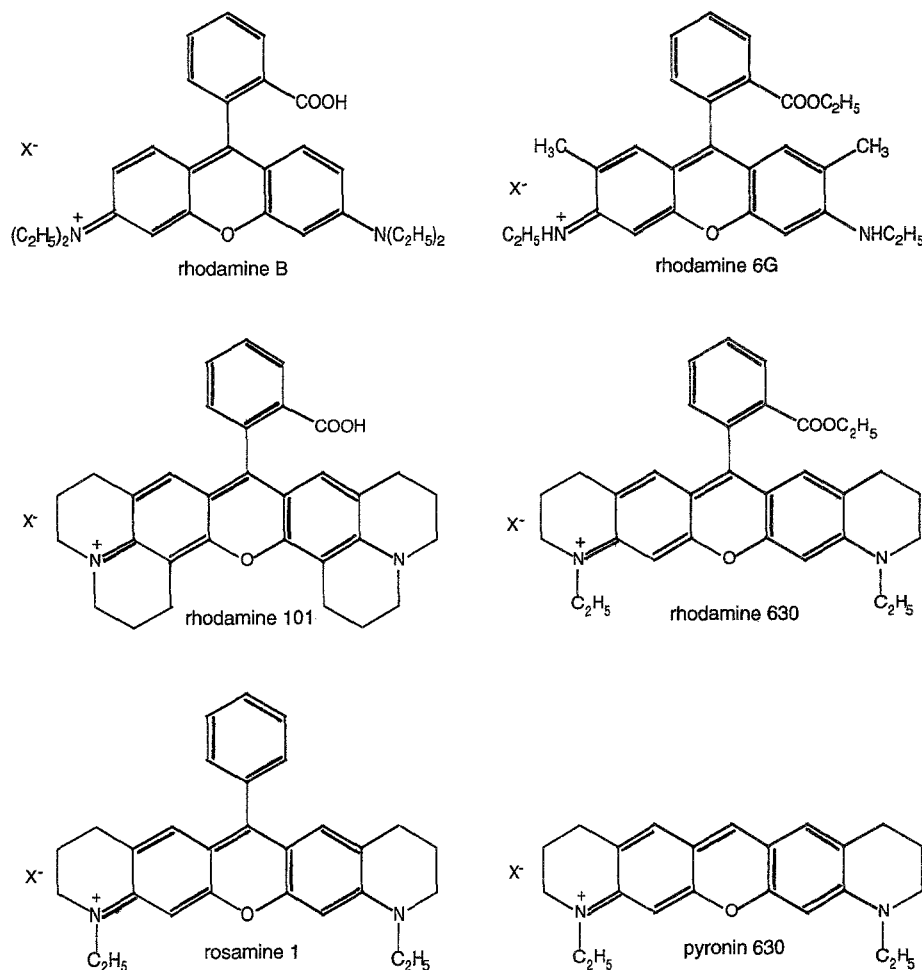


Fig. 2. Molecular structures of rhodamine B, rhodamine 6G, rhodamine 101, rhodamine 630, rosamine 1, and pyronin 630.

ity in the first excited state. This process results in a state with charge transfer character and reduced $S_1 - S_0$ energy gap. Hence the internal conversion rate increases as demonstrated by a reduced fluorescence efficiency and decay time. In this double-potential minimum model the height of the potential barrier and the energy difference between the initial and the final states are controlled by solvent viscosity and polarity as well as by steric and electronic properties of the phenyl substituent and the xanthene chromophore.⁽¹¹⁾

Typically in fluorescent DNA-sequencing techniques and immunoassays the rhodamine or fluorescein labels are characterized by different emission spectra. The selectivity is obtained by positioning suitable band-pass filters in front of the detector. The identification is based on a multicomponent analysis of fluorescence intensity measurements, recorded through the different bandpass filters. The number, position, and bandwidth

of the filters determine the sensitivity and selectivity of the detection. Meanwhile in routine diagnostics there is a growing need for multianalyte (multiparameter) analysis. However, the present methodology does not allow the use of more than three or four simultaneous labels because the spectrometric separation of the signals from different labels is not sufficiently efficient. As the emission spectra of different fluorescent labels overlap significantly, the identification of a particular label is difficult.

To increase the number of discernible fluorescent labels we have developed a new concept. The method is based on labeling the molecules or material under investigation with different fluorescence lifetimes. Hence, not only can the spectral information of the dye be utilized, but so can the characteristic fluorescence lifetime. In addition, time-resolved detection allows the separation of fluorescence from Rayleigh-scattered excitation

Table I. Spectroscopic Characteristics of Rhodamine B, Rhodamine 6G, Rhodamine 101, Rhodamine 630, Rosamine 1 [12], and Pyronin 630 at 25°C^a

Dye	Aqueous buffer, pH 3.0			Ethanol (H ⁺) ^b			Φ_f
	λ_{abs} (nm)	λ_{em} (nm)	τ (ns)	λ_{abs} (nm)	λ_{em} (nm)	τ (ns)	
Rhodamine B	557	578	1.43	552	579	2.28	0.55
Rhodamine 6G	526	556	3.89	530	556	3.79	0.95
Rhodamine 101	579	608	4.17	574	601	4.28	0.92
Rhodamine 630	564	588	4.04	563	587	4.06	0.97
Rosamine 1	565	592	2.68	562	589	3.76	0.88
Pyronin 630	559	579	3.69	559	579	3.72	0.92

^a Extinction coefficient at the absorption maximum has the values 1.12×10^5 and 1.24×10^5 L mol⁻¹ cm⁻¹ for ethanolic solutions of rhodamine 6G and rhodamine 630, respectively.

^b To ensure protonation of rhodamine B and rhodamine 101, a drop of trifluoroacetic acid was added to 1 ml of the alcoholic dye solution.

light by suitable gating. Besides the straylight, another background source in low-level detection experiments that can be discriminated against by gated time-resolved detection techniques is water Raman scattering, which occurs simultaneously with the excitation light at a fixed frequency shift. In order to excite different dyes efficiently with a single monochromatic light source we have developed fluorescent dyes whose absorption and emission wavelengths are nearly identical, which differ, however, in fluorescence lifetime. Fluorescent dyes with these characteristics are called “multiplex dyes”.^(10–14,4) In combination with a pattern recognition technique, only a rather small number of photons have to be collected for high-precision identification of the fluorescent label.^(14,15) Using highly repetitive laser systems (>10 MHz) and fast signal processing, the identification time per fluorescent dye is in the range of milliseconds. To label the analytes with unequivocal fluorescence lifetimes, it is desirable to use dyes which show fluorescence properties nearly independent of the molecular environment. For that reason we started our investigations with a group of dyes derived from rhodamine 630, in which the amino groups are incorporated in rigid six-membered rings (Fig. 2).

Difficulties may arise due to the fact that the absorption maxima of these rhodamines are well below 600 nm. Fluorescence detection sensitivity in this wavelength range can be severely compromised by back-

ground signals caused by the autofluorescence of the probe. Samples that include serum show a fairly strong fluorescence of their own in the region of most fluorescent probes (Fig. 3). In addition to the serum's own fluorescence, the background is enhanced by strong scattering, which results from proteins and other macromolecular compounds. This difficulty as well as the advent of low-cost optical sources and detectors in the visible–near-IR region have prompted our efforts to develop multiplex dyes with absorption and emission beyond 600 nm.

In this communication we report on the development of new highly fluorescent dyes with absorption and emission beyond 600 nm for time-resolved detection with laser diodes.

EXPERIMENTAL

Details of the dye preparation are published in Refs. 16 and 17. Reversed-phase HPLC with a gradient of 0–75% acetonitrile in 0.1 M aqueous triethyl ammonium acetate (TEAA) was used for the purification of the rhodamines.

Synthesis of Dye-Labeled 3'-Deoxy-Amino-Thymidine

Synthesis of 3'-deoxy-amino-thymidine is described in Ref. 18. The coupling reaction between the *in situ* activated carboxyrhodamine derivatives (succinimido esters) and the amino-modified thymidine was carried out in dimethyl formamide (DMF).^(19,20) Amino-nucleoside and carboxyrhodamine (1:1) were taken up in DMF. After addition of N,N,N',N'-tetramethyl (succinimido)uronium tetrafluoroborate (TSTU) (Fluka) and N,N-diisopropylethylamin (Fluka) (each 1.5-fold), the reaction was performed for 12–14 h in the dark at room temperature. Reversed-phase HPLC with a gradient of 0–75% acetonitrile in 0.1 M aqueous triethyl ammonium acetate (TEAA) was used for the purification of the product.

Synthesis of Dye-Labeled Oligonucleotides

The oligonucleotides (Roth) were modified at their terminus using 5'-amino-modifier C₆ (Glen Research). An aliquot (10 μ l) of these oligonucleotides was dissolved in sterile water (18 nmol) and the following reagents were added in order: 20 μ l of TSTU (10 mg/ml dimethylformamide, Fluka), 5 μ l of dye (5 mg/ml dimethylformamide), 20 μ l of DMF, and 2 μ l of diisopropylethylamine. The solution was incubated overnight in

⁴ The structure of the dye JA32⁽¹³⁾ has to be corrected: C₃F₇ instead of C₃H₇.

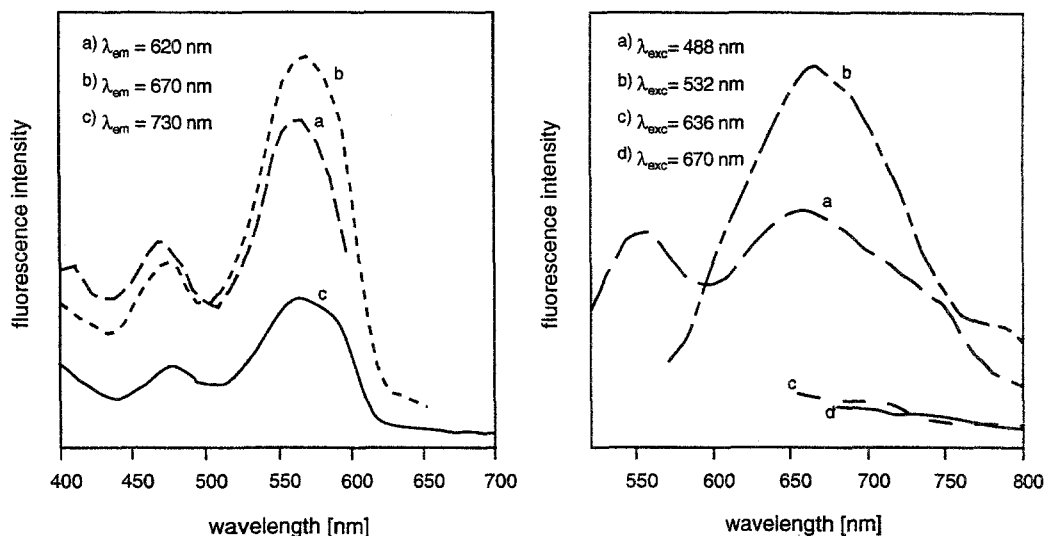


Fig. 3. Fluorescence excitation (left) and emission spectra (right) of a human serum probe at different emission and excitation wavelengths, diluted 1:100 with bidistilled water.

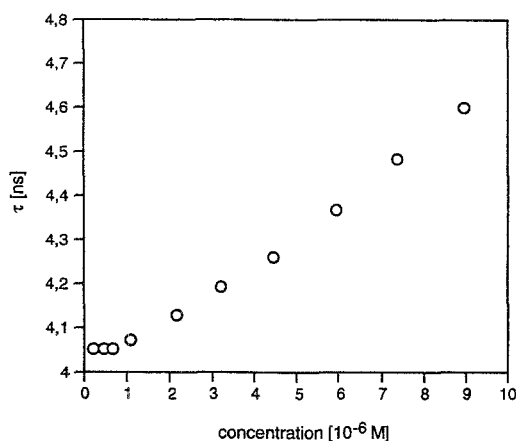


Fig. 4. Measured fluorescence lifetime τ of rhodamine 630 in ethanol at different concentrations. Fluorescence signal was detected perpendicular to the direction of excitation in a standard quartz cuvette (path-length 10 mm).

the dark and the labeled oligonucleotides were purified by reversed-phase HPLC. All solvents—not degassed—were spectroscopic grade (Aldrich) and used without further purification. Measurements in aqueous systems were performed using the following buffers: 100 mM citrate buffer, pH 3.0; 100 mM phosphate buffer, pH 7.0; and 100 mM tris-borate buffer, pH 8.4, containing 7 M urea (Beckman). The latter is the aqueous medium for polyacrylamide gels used in DNA sequencing. The aqueous buffers pH 8.0, 9.0, and 10.5 were 100 mM tris buffer, adjusted with HCl.

The dye concentration was kept strictly below 10^{-6} M in all solutions. Low concentration is important because of the considerable overlap of absorption and fluorescence spectra (Fig. 1). In concentrated solutions this leads to prolongation of the measured fluorescence decay due to reabsorption and reemission of fluorescence photons (Fig. 4). As can be seen from the figure, no self-absorption and self-emission occurs at concentrations $<10^{-6}$ M. Published values of decay times for xanthene dyes vary enormously, which might result, at least in part, from insufficient attention to the problem indicated above.⁽²¹⁾

Rhodamine B, rhodamine 6G, rhodamine 101, rhodamine 630, rosamine 1, and pyronin 630 were measured with a hydrogen-filled flashlamp (1.5 ns FWHM), using a time-correlated single-photon counting technique with an instrument from PTI (Model LS100). The samples were excited at the long-wavelength maximum. The fluorescence decay was monitored at the emission maximum. The rhodamine derivatives having absorption maxima above 600 nm were excited with a pulsed laser diode (Hamamatsu PLP01, 636 nm, 10 μ W, 100 ps FWHM, 10 MHz repetition rate), using time-correlated a single-photon counting technique. A PMT from the lifetime spectrometer LS100 (PTI) was used for detection together with the necessary electronic equipment. The measurements were carried out in the reverse mode, i.e., the start pulses were provided by the PMT.

Time-resolved measurements in capillaries were done with the pulsed laser diode. The laser was mounted

onto a micrometer two-dimensional translation stage and illuminated the capillary (fused silica capillary with 360 μm o.d. and 200 μm i.d.) from above. The fluorescence signal was detected perpendicular to the direction of excitation and to the direction of the capillary after passing a bandpass filter (CWL 670 nm, FWHM 12 nm). In these measurements the dye concentration was below 10^{-8} M.

The instrument response function needed for deconvolution was obtained from a scattering solution. The quality of the decay fits were controlled by the reduced chi-squared statistical parameter. Most of the decays could be described satisfactorily by a monoexponential model ($\chi^2 < 1.2$). In the cases where a second component was necessary a biexponential model was used to fit the decay:

$$I(t) = a_1 \exp(-t/\tau_1) + a_2 \exp(-t/\tau_2) \quad (1)$$

where a_1 and a_2 are preexponential factors, which describe the ratio of the excited species ($a_1 + a_2 = 1$), and τ_1 and τ_2 denote their lifetimes. The fluorescence quantum yield was measured using a thermal blooming technique.⁽²²⁾

The redox potentials were determined by cyclic voltammetry (CV) in dry acetonitrile purchased from Aldrich. Tetra-*n*-butylammonium hexafluorophosphate ([TBA]PF₆, Merck) was used as the supporting electrolyte. The 0.1 M solutions of the electrolyte were purified and dried using neutral aluminum oxide (ICN alumina N, super I). Measurements were performed in a three-electrode arrangement in a single cell at 20°C. The scan speed was 100 mV/s. The positive and negative voltage limits of this system are +2.4 V and -2.8 V vs SCE in acetonitrile.

RESULTS AND DISCUSSION

Although the composition of human plasma will strongly depend on the individual source, the excitation and emission spectra of Fig. 3 show that the fluorescent background can be greatly minimized by exciting the sample at a wavelength above 620 nm. Therefore it would be desirable in biodiagnostics to work with fluorescent labels that can be easily coupled to the analyte, absorb in the visible-near-IR region, and show a high fluorescence efficiency in aqueous environment. Here a difficulty arises due to the fact that at longer absorption wavelengths the fluorescence efficiency tends to decrease with decreasing energy difference between S_1 and S_0 . In particular, hydrogen vibrations lead to a decreased

quantum yield in the red-near-IR region. The quanta of hydrogen stretching vibrations have the highest energies in organic compounds. Thus hydrogen vibrations are most likely to contribute to internal conversion between S_1 and S_0 . This mechanism, which is expected only for those hydrogens that are attached directly to the chromophore,⁽⁸⁾ is of minor importance in dyes that emit in the visible range. However, it can seriously reduce the fluorescence efficiency of infrared dyes. In view of these limitations it would be desirable to work with excitation wavelengths as short as possible. Unfortunately, relatively few fluorescent dyes with sufficient fluorescence quantum yields that absorb at wavelengths above 620 nm are known, and fewer still are available in reactive form for conjugation with biomolecules. The available long-wavelength dyes consist primarily of cyanine derivatives with various reactive groups.⁽²³⁻²⁶⁾ Hence we have investigated the possibility of utilizing new rhodamine dyes in the wavelength region 630-700 nm (Figs. 5 and 6).

It has been known for a long time that if the central carbon group of a pyronin or rhodamine dye is replaced by a nitrogen atom, a compound is obtained whose absorption and emission are shifted by about 100 nm to longer wavelengths.⁽²⁷⁾ Such planar oxazine derivatives are rigid and exhibit suitable spectroscopic characteristics in the wavelength region 580-700 nm. The exchange of the carboxyphenyl substituent by an electron-accepting group at the central carbon of the rhodamine has an effect similar to the introduction of a nitrogen atom. In the case of a cyano group the resulting rhodamine derivative exhibits absorption and emission spectra shifted by about 100 nm (compare rhodamine 101 and rhodamine 800, Tables I and II). The squares of frontier orbital coefficients calculated with semiempirical methods show that the electron density at the central carbon of a pyronin chromophore is zero in the HOMO but high in the LUMO. By introduction of an electron acceptor at this position or exchange of the methine group by a more electronegative atom the energy of the LUMO will decrease, resulting in a decreased excitation energy.

Another possibility to shift the absorption maximum toward longer wavelengths is the addition of two double bonds. This is demonstrated by the dyes JA 22 and JA 93 (Fig. 5). Due to the two additional double bonds in the nitrogen-containing rings, the absorption and emission maxima exhibit a shift to longer wavelengths of about 30 nm (Fig. 6 and Table II). The different absorption wavelengths of the dyes JA 105 and JA 106 cannot be explained with any existing model. The absorption and

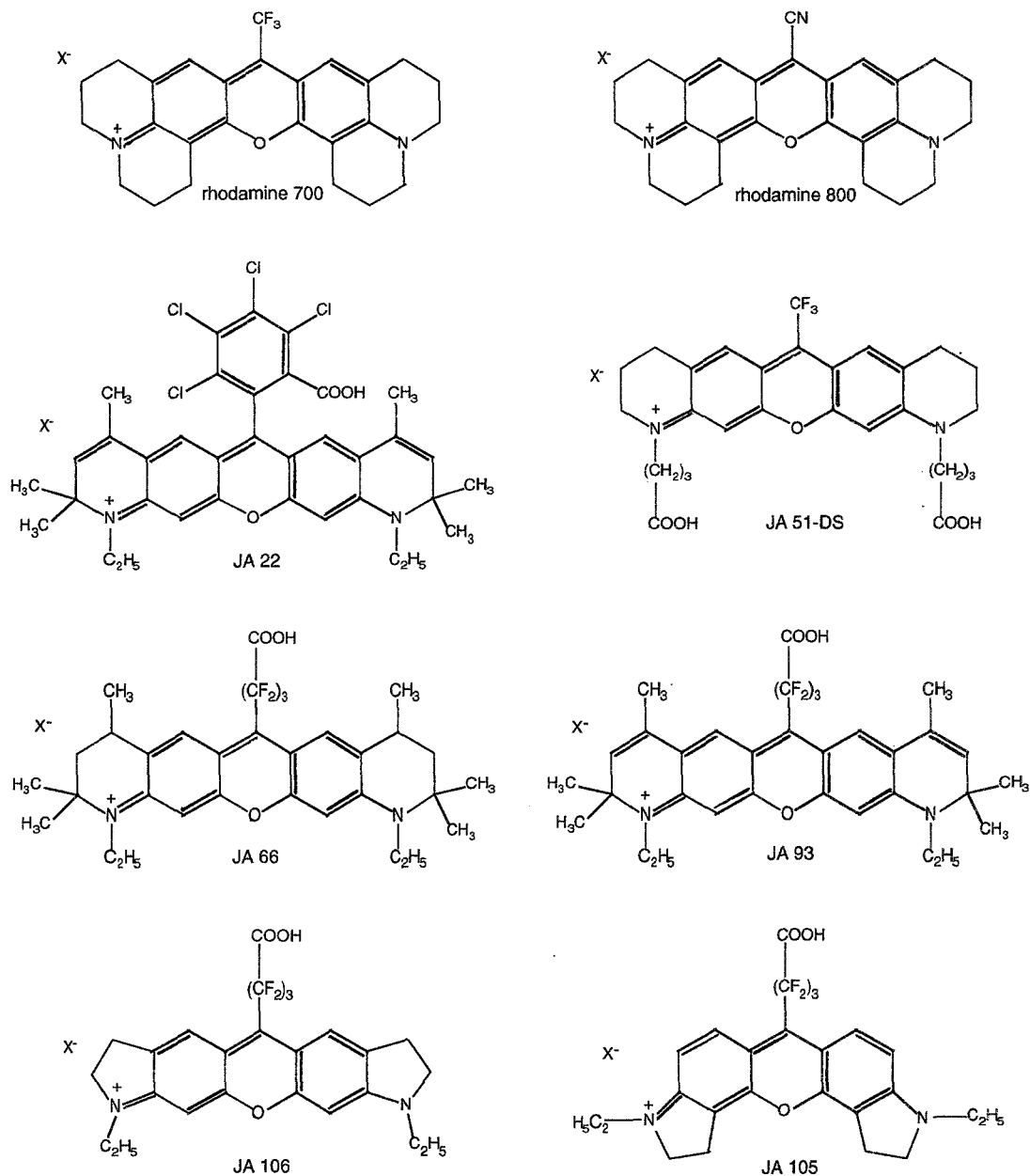


Fig. 5. Molecular structures of new rhodamine derivatives with absorption and emission above 600 nm (for comparison the commercially available rhodamine 700 and rhodamine 800 are shown).

emission maxima show a peculiar dependence on the position of the five-membered rings. The difference in absorption between the two isomers is about 45 nm. Additionally the fluorescence decay time and quantum yield of JA 105 is less than half the decay time and quantum yield of JA 106 (Table II and Fig. 6c). This great difference in quantum yield cannot be attributed simply to a higher internal conversion rate due to a smaller energy gap between S_1 and S_0 .

The data of Table II demonstrate that the new rhodamine derivatives are well suited for a time-resolved detection. Tables II and III indicate that the lifetimes of the rhodamine dyes are adequately long to allow the use of simple instrumentation. The single-photon counting measurements can be performed with laser diodes for excitation and photoavalanche diodes or photomultiplier tubes for detection and do not require more complex designs using high-speed detectors. Recently it has be-

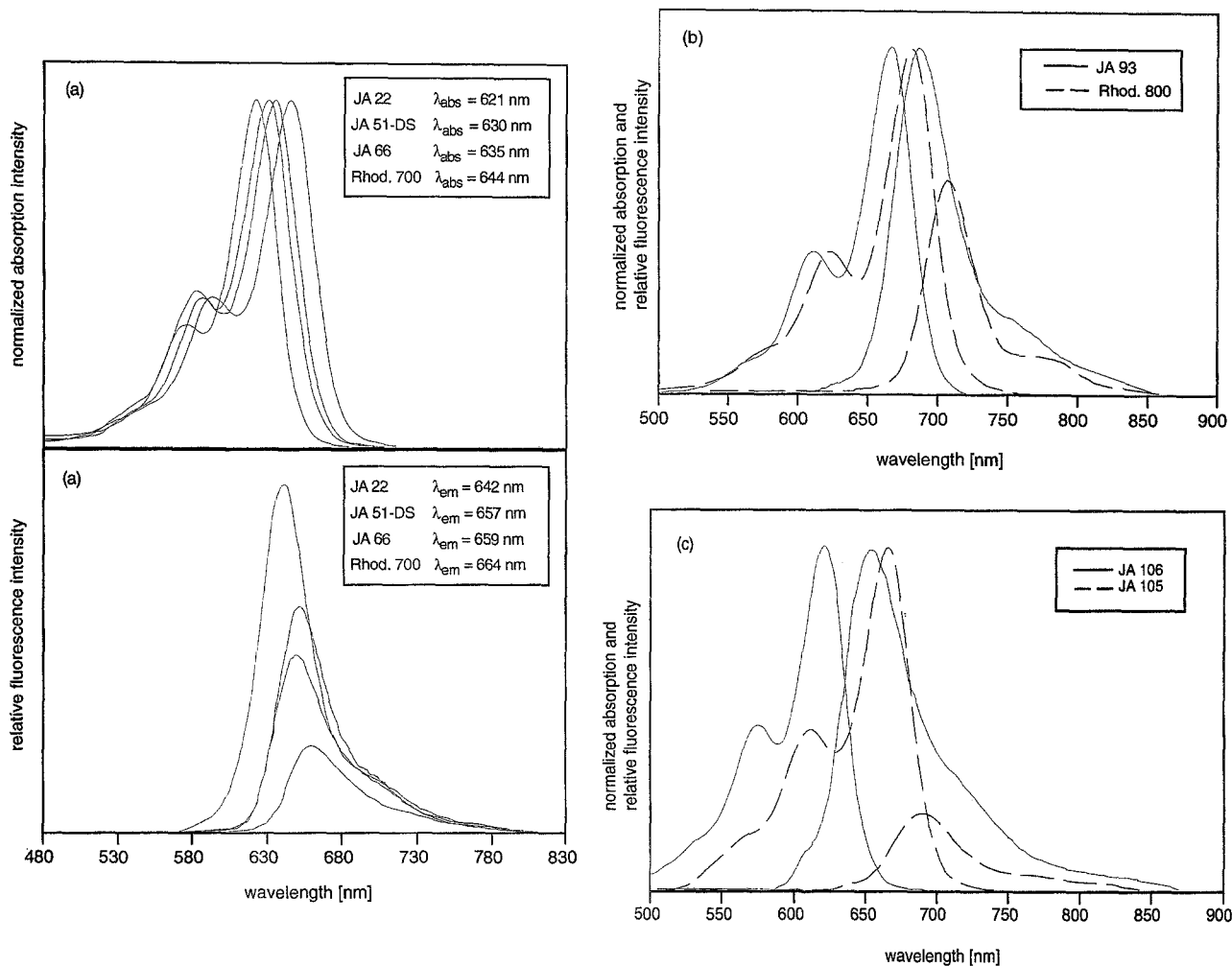


Fig. 6. Normalized absorption and relative emission spectra of (a) JA 22, JA 51-DS, JA 66, rhodamine 700, (b) JA 93, rhodamine 800, (c) JA 105 and JA 106 in ethanol. To ensure protonation and prevention of the pseudobase formation, a drop of trifluoric acid was added to 1 ml of the dye solution. The relative fluorescence intensities clearly demonstrate that the new rhodamine derivatives exhibit higher fluorescence quantum yields compared with the commercially available rhodamine 700 and rhodamine 800.

come possible to locate the total signal processing on a PC interface card. Hence the required system is compact and inexpensive.

Because in the new dyes the amino groups are incorporated in a single rigid ring it is easily possible to attach a functional group for covalent coupling of analytes. This is exemplified by the dye JA 51-DS. Besides the capability of covalent coupling to analytes, the new rhodamines exhibit higher quantum yields and lifetimes than the commercially available rhodamine 700 and rhodamine 800 in this wavelength region (Table II and Figs. 6a and 6b). The fluorescence quantum yield of JA 22 has the value 0.92 in basic and 0.90 in acidic ethanol. Although the new rhodamines exhibit a rather small

Stokes shift, the high fluorescence quantum yields allow a sensitive fluorescence detection even outside the emission maximum.

In order to optimize the coupling efficiency we investigated the influence of the length of the carbon chain between the chromophore and the carboxyl group on the yield of the coupling reaction with 3'-deoxy-amino-thymidine. The dyes of Fig. 7 contain the same rhodamine chromophore ($\Phi_f = 0.95$). They vary, however, in the size of the coupling substituent. We achieved the highest coupling yield (95%) with the dye carrying $-\text{CH}_2\text{-COOH}$ substituents (Fig. 7a). With increasing length of the coupling substituent the yield decreases. The dye with $-\text{CH}_2\text{-CH}_2\text{-COOH}$ substituents (Fig. 7b) yielded 50%

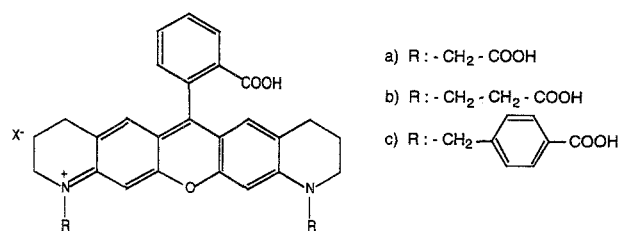
Table II. Spectroscopic Characteristics of Rhodamine Derivatives with Absorption and Emission Above 600 nm in Ethanol^a

Dye	λ_{abs} (nm)	λ_{em} (nm)	τ (ns)	Φ_f (%)
Rhodamine 700	644	664	2.65	36
Rhodamine 800	682	698	2.07	19
JA 22	621	642	4.06	90
JA 51-DS	630	657	3.41	54
JA 66	635	659	3.89	70
JA 93	667	691	3.43	56
JA 106	623	649	3.08	
JA 105	669	694	1.39	

^a Extinction coefficient at the absorption maximum values 1.10×10^5 , 0.97×10^5 , and 1.02×10^5 L mol⁻¹ cm⁻¹ for ethanolic solutions of JA 22, JA 51-DS, and JA 93, respectively. To ensure protonation and prevention of the pseudobase formation, a drop of trifluoroacetic acid was added to 1 ml of the alcoholic solution of JA 22, JA 51-DS, JA 66, JA 93, JA 106, and JA 107.

Table III. Fluorescence Lifetimes τ (ns) of the New Rhodamine Derivatives JA 22, JA 66, and JA 51-DS in Various Solvents Without Addition of Trifluoroacetic acid

	JA 22	JA 66	JA 51-DS
Ethanol	4.06	3.89	3.41
Glycerol	3.88	3.72	2.89
Methanol	4.13	3.99	3.35
Formamide	3.9	3.84	3.55
Trifluoroethanol	4.73	4.58	4.37
Aqueous buffer, pH 7.0	3.62	2.35	2.16
7 M urea	3.83	2.82	2.37

**Fig. 7.** Rhodamine dyes with various substituents R for coupling. Using the dye with R = CH₂-COOH gave a coupling efficiency of 95% with 3'-deoxy-amino-thymidine.

product. In case of the *p*-benzoic acid derivative (Fig. 7c) only a very small yield of 10% was achieved in the coupling reaction.

To test the applicability of the new rhodamines for biagnostics in aqueous environment we studied the spectroscopic characteristics of these dyes also in aque-

ous buffer systems. As mentioned earlier,^(11,12) almost all rhodamines absorbing above 600 nm show a marked decrease in fluorescence lifetime on changing from ethanol to aqueous environment. Exceptions are dyes derived from JA 22. The fluorescence lifetime of this dye is shortened only slightly in aqueous systems (Table III). In order to investigate the solvent dependence further, we measured the fluorescence lifetime of the new rhodamines in other water-related solvents such as formamide, trifluoroethanol, methanol, and glycerol. As indicated by the data of JA 66 and JA 51-DS (Table III), the rhodamines with perfluoroalkyl substituents at the central carbon exhibit a long fluorescence lifetime in all observed solutions, except aqueous environment. The rhodamine derivative JA 22 with the tetrachlorocarboxyphenyl substituent shows fluorescence efficiency near unity also in aqueous buffer. The exceptionally long lifetimes in trifluoroethanol can be explained by the small refractive index of this solvent. As shown above for the case of pyronin 630, the loss of the carboxyphenyl substituent has only small influence on the fluorescence lifetime (Table I), even in aqueous buffer. Hence we assume that the decrease of lifetime in water is connected with the electron-accepting properties of the perfluoroalkyl substituent at the central carbon, which reduce the electron density of the LUMO. Interestingly, the fluorescence lifetime in aqueous solution increases on addition of 7 M urea. This is important, as this environment is used in DNA-sequencing experiments.

In hydrogen bonding solvents such as alcohols or water the rhodamine dyes are present in their dissociated ionic forms and are solvated mostly through their oxygen and nitrogen atoms. Due to the solvation of the rhodamine cations the repulsive electrostatic interactions decrease, thus promoting the aggregation tendency. It is well known that xanthene dyes have the tendency to form dimers in aqueous solution which show a strong absorption band at wavelengths shorter than the monomers.^(8,28-31) Furthermore, the dimers are generally non-fluorescent, indicated also by a monoexponential fluorescence decay measured at high concentrations in water. It is possible to suppress the aggregation of dyes in aqueous solution either by increasing the hydrophilic properties of the dye by additional sulfonate or carboxyl groups or the addition of organic compounds such as *N,N*-dimethyldodecylamine-*N*-oxide, sodium lauryl sulfate, triethyl ammonium chloride, or urea. While compounds such as sodium lauryl sulfate promote the formation of micelles, the role of urea is not yet clearly understood. Apparently urea replaces water molecules around the hydrophobic dye, causing a change in solvation of the latter, also demonstrated by a bathochromic

Table IV. Spectroscopic Characteristics of the Free and Coupled Dyes MR 200-1 and JA 51-DS^{a,b}

	MR 200-1	MR 200-1-N ₁₇	MR 200-1-N ₁₈	JA 51-DS	JA 51-DS-N ₁₇	JA 51-DS-N ₁₈
λ_{abs} (nm)	618/622	622/622	622/622	628/634	638/638	638/638
λ_{em} (nm)	638/642	639/639	639/639	654/659	659/659	659/659
τ_1 (ns)	3.62/3.83	4.08/4.03	4.06/4.05	2.16/2.41	0.53/1.08	0.51/1.10
τ_2 (ns)	—	—	—	—	3.05/3.08	2.99/2.91
a_1	1.00	1.00	1.00	1.00	0.54/0.18	0.41/0.10

^a First value is for the dye in 100 mM phosphate buffer, pH 7.0; second value is for the dye in 100 mM tris-borate buffer, 7 M urea, pH 8.4. Samples were excited with a pulsed laser diode emitting at 636 nm, and the emission was detected through a bandpass filter (CWL 670 nm).

^b N₁₇: 5'-GTT TTC CCA GTC ACG AC-3'. N₁₈: 5'-TGT AAA ACG ACG GCC AGT-3'.

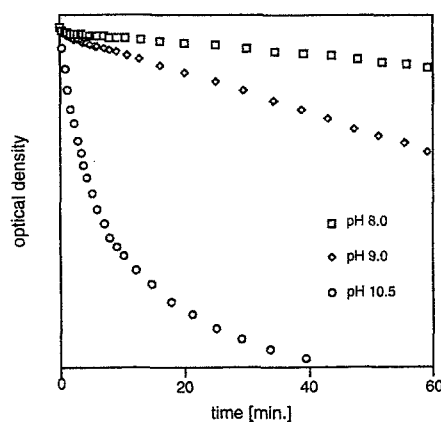


Fig. 8. Loss of absorption of an aqueous buffered JA 51-DS solution with time at different pH values. The reaction rate for the nucleophilic attack of the hydroxide ions depends on the pH of the solution. After 2 h in the basic medium the formation of the pseudobase is still completely reversible by adding of one drop trifluoroacetic acid to 1 ml of dye solution. At longer periods of exposure to basic conditions the dye does not recover completely.

shift in absorption and emission as well as by the longer lifetime (Table IV). Therefore these dyes are well suited for time-resolved DNA-sequencing methods using gel-filled capillaries, containing a 7 M urea tris-borate buffer as aqueous medium.

An interesting phenomenon is the loss of absorption and emission frequently observed in coupling experiments with rhodamine derivatives absorbing above 600 nm. Most coupling reactions to amino groups are carried out under basic conditions. Unfortunately, all triphenylmethane and related dyes show a tendency to react at the central carbon with nucleophiles, e.g., hydroxide ions, if this carbon is sterically available. Thus a dye such as pyronin 630 (Fig. 2) becomes colorless on addition of a base to its aqueous solution, owing to the formation of a so-called pseudobase. In the pseudobase the π -electron system is interrupted and therefore the long-wavelength absorption is lost. Although this pro-

cess is reversible, subsequent reactions (e.g., oxidation) may lead to an irreversible destruction of the dye. This reaction does not occur in normal rhodamines, because the central carbon of the chromophore is protected by the carboxyphenyl substituent. Among our new dyes the pseudobase formation is not possible in the case of JA 22. This dye is completely stable even in strongly basic solutions. On the other hand, those dyes that carry electron-accepting groups at the central carbon such as cyano or perfluoroalkyl substituents will form a pseudobase depending on the pH of the solution (Fig. 8). Not only the equilibrium constant, but also the rate constant for the nucleophilic attack of the hydroxide ions depends on the proton concentration as well as on the environment. However, the nucleophilic attack can be slowed down by the addition of urea. As mentioned above, no formation of dimers in aqueous solutions could be observed in concentrations up to 10^{-6} M by addition of 7 M urea. Interestingly, also no loss of absorption or fluorescence intensity is observed even after many hours.

As demonstrated by our experiments, the rhodamine derivative JA 22 is well suited for ultrasensitive fluorescence detection using laser diodes as excitation source. Unfortunately, the absorption maximum of this dye occurs at 620 nm, which is outside the wavelength range of diode lasers commercially available today. Working with a diode laser emitting at 636 nm, about 30% of the excitation efficiency is lost. Additionally the detection wavelength has to be shifted to longer wavelengths to block the stray light. Due to the small Stokes shift of rhodamines, the detection sensitivity is rather small. However, it can be expected that the wavelength range of powerful diode lasers will be extended to shorter wavelengths in the near future.

To couple the dye JA 22 to amino functions of modified DNA bases, oligonucleotides, or antibodies we replaced one ethyl group of the dye by a $-\text{CH}_2-\text{COOH}$ group. This has practically no influence on the spectro-

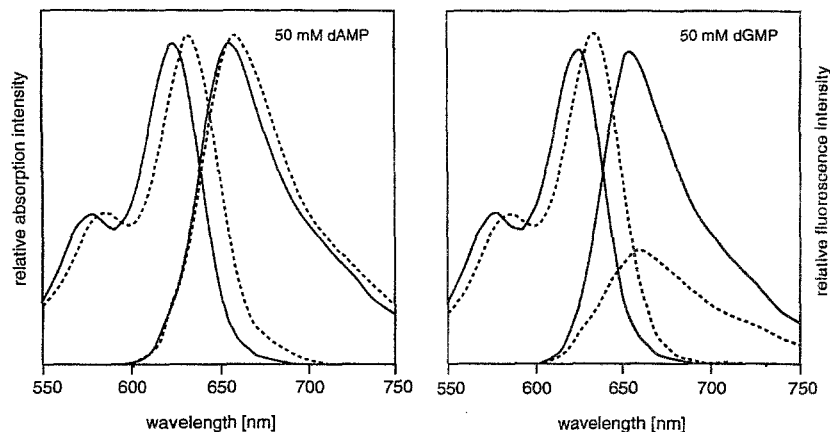


Fig. 9. Absorption and emission spectrum of JA 51-DS in 100 mM phosphate buffer, pH 7.0, without addition of nucleotides (solid curve), and in solution containing 50 mM 2'-deoxyadenosine-5'-monophosphate (dAMP) and 50 mM 2'-deoxyguanosine-5'-monophosphate (dGMP) (- -).

scopic characteristics. As indicated in Table IV, the rhodamine derivatives JA 51-DS and the modified JA 22 (MR 200-1) can both be excited with the same diode laser emitting at 636 nm and exhibit sufficient differences in their excited-state lifetime. Hence we can use the fluorescence lifetime for an unequivocal identification of the dye.

To prove the applicability of these two dyes for time-resolved DNA-sequencing techniques, we coupled them to synthetic oligonucleotides using a C_6 -amino-linker. Such oligonucleotides are used as primers in Sanger's enzymatic DNA-sequencing method.⁽³²⁾ Due to the basic coupling conditions the dye JA 51-DS loses its color during the reaction with the amino group of the linker. After the reaction the purified colorless solution was quickly freeze-dried and stored at -20°C . After warming up to room temperature 5 μl of a diluted HCl solution of pH 1.0 was added. Within 30 min the chromophoric system recovered and the concentrated solution was diluted with the respective aqueous buffer.

Using a cooled laser diode as excitation source ($\lambda_{\text{em}} = 632 \text{ nm}$), we could demonstrate the fluorescence-based detection of oligonucleotides in a commercially available capillary electrophoresis system under realistic DNA-sequencing conditions.^(12,33) Table IV presents the spectroscopic characteristics of the coupled dyes in 100 mM phosphate buffer, pH 7.0, and 100 mM tris-borate buffer, containing 7 M urea, pH 8.4. As mentioned above, both dyes show bathochromic shifts in absorption and emission, and exhibit a longer fluorescence lifetime by adding 7 M urea to aqueous solutions. The coupling of MR 200-1 to oligonucleotides has very little influence on the spectroscopic characteristics of the chromophore. The fluorescence quantum yield and lifetime increase,

whereas the absorption and emission maxima show only very small shifts.

The free dye JA 51-DS exhibits a monoexponential fluorescence decay in aqueous buffered solutions. However, when this dye is linked to the oligonucleotides, the fluorescence kinetics indicates the presence of at least two lifetimes: a shorter and a longer component compared with the decay time of the free dye (Table IV). In phosphate buffer the absorption and emission maxima are shifted to longer wavelengths, while in 7 M urea only the absorption maximum shows a bathochromic shift in the conjugates. Comparison of the relative fluorescence quantum yields of the free and coupled dye JA 51-DS demonstrates that the fluorescence intensity in the conjugates is reduced by about 30–40% in phosphate buffer and by only 10–20% in 7 M urea.

From intermolecular quenching experiments with JA 51-DS and 2'-deoxynucleotide-5'-monophosphates (dNMP) in aqueous medium we deduce that the DNA base guanosine is responsible for the observed fluorescence quenching. On addition of purine bases (dAMP, dGMP) in phosphate buffer the absorption maximum shifts to longer wavelengths (10 nm) and the optical density increases slightly, indicating ground-state interactions between the dye and the purine bases (Fig. 9). The emission maximum shows a smaller shift of only 4–5 nm. With the two pyrimidine bases (dCMP, TMP) similar but smaller effects are detected. On addition of adenosine, cytosine, or thymidine the fluorescence intensity and lifetime of JA 51-DS increase, whereas guanosine causes a drastic decrease in fluorescence intensity (Fig. 9). Furthermore, the Stern–Volmer plots obtained from steady-state quenching experiments in 100 mM phosphate buffer, pH 7.0, are characterized by a downward

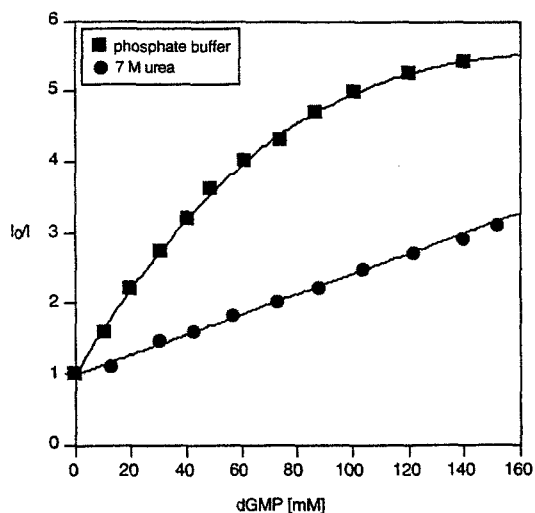


Fig. 10. Relative fluorescence intensities of JA 51-DS with increasing concentrations of 2'-deoxyguanosine-5'-monophosphate (dGMP) in 100 mM phosphate buffer, pH 7.0, and 100 mM tris-borate buffer, pH 8.4, containing 7 M urea. I_0 is the intensity in the absence of dGMP, and I is the same value with addition of dGMP.

Table V. Biexponential Intensity Decay Analysis of JA 51-DS with Different 2'-Deoxyguanosine-5'-Monophosphate (dGMP) Concentrations in Aqueous Buffer Systems^a

	dGMP (mM)	τ_1 (ns)	τ_2 (ns)	a_1	a_2	χ^2
100 mM Phosphate buffer, pH 7.0	0	—	2.16	—	1.00	1.10
	10	0.53	2.06	0.28	0.72	1.06
	32	0.53	1.95	0.49	0.51	1.15
	47	0.53	1.86	0.56	0.44	1.00
	63	0.53	1.79	0.65	0.35	1.08
100 mM tris-Borate buffer, 7 M urea, pH 8.4	0	—	2.41	—	1.00	1.05
	9	1.10	2.37	0.03	0.97	1.10
	26	1.10	2.34	0.12	0.88	1.14
	47	1.10	2.29	0.23	0.77	1.06
	70	1.10	2.25	0.39	0.61	1.01

^a Data were fitted with a constant short lifetime τ_1 . Samples were excited at 620 nm with a hydrogen-filled flashlamp from the PTI spectrometer. Emission was recorded at 650 nm.

curvature, indicating at least two populations of fluorophores (Fig. 10).

On addition of 2'-deoxyguanosine-5'-monophosphate (dGMP) to an aqueous solution of JA 51-DS the fluorescence decay kinetics demonstrates that a multiexponential model is necessary for a satisfactory description of the decays. We obtained the best results using a biexponential fit with a short lifetime independent of the quencher concentration (in 100 mM phosphate buffer, pH 7.0, $\tau_1 = 0.53$ ns; in 7 M urea, $\tau_1 = 1.10$ ns) and

Table VI. Amplitudes of a Global Analysis of the Intensity Decays of Aqueous Buffered Solution of JA 51-DS with 50 mM dGMP Measured at Different Excitation (λ_{exc}) and Constant Emission Wavelength ($\lambda_{em} = 660$ nm)^a

λ_{exc} (nm)	610	620	630	640
a_1	0.54	0.57	0.69	0.74
a_2	0.46	0.43	0.31	0.26

^a Samples were excited with the hydrogen-filled flashlamp from the PTI spectrometer. The analysis reveals two lifetimes of $\tau_1 = 0.53$ ns and $\tau_2 = 1.78$ ns independent of the excitation wavelength.

another longer lifetime decreasing linear with increasing quencher concentration (Table V). From the linear Stern–Volmer plots of the concentration-dependent second lifetime τ_2 we determine bimolecular quenching rate constants $k_q = 1.4 \times 10^9 M^{-1} s^{-1}$ in 100 mM phosphate buffer, pH 7.0, and $k_q = 0.4 \times 10^9 M^{-1} s^{-1}$ in 7 M urea, pH 8.4. As indicated by the data in Table V, the amplitude a_1 of the constant lifetime τ_1 increases with increasing quencher concentration. In 7 M urea the complexation tendency is reduced and therefore the amplitudes a_1 corresponding to the fluorescent ground-state complexes (Table V) and also the rates of dynamic quenching are reduced. The observed behavior leads to the conclusion that the effects responsible for the aggregation of dye molecules in water occur also with 2'-deoxynucleotide-5'-monophosphates. In the conjugates (Table IV) the dye is coupled through a C₆-aminolinker to the 5'-end of the oligonucleotide chain. Due to the conformational flexibility of the linker and the tendency of nonpolar species to aggregate in water so as to decrease the hydrocarbon–water interfacial area, an interaction between the dye and the hydrophobic part of the nucleotides is possible. Therefore ground-state complexes are formed whereby the absorption maximum shifts to longer wavelengths with slightly increased extinction. Therefore the amplitudes derived from a biexponential fit are strongly dependent on the chosen excitation wavelength. Table VI shows the global analysis of the intensity decays of a phosphate-buffered solution of JA 51-DS containing 50 mM dGMP, measured at different excitation wavelengths. The global analysis reveals two decay times of $\tau_1 = 0.53$ ns and $\tau_2 = 1.78$ ns at all excitation wavelengths (Table VI). Because of the lower fluorescence quantum yield and lifetime of the ground-state complex compared to the free dye in water, the fractional intensity of the free component will be the dominant component in the decay time measurements. Hence, the emission maximum shows only a smaller shift to longer wavelengths (Fig. 9 and Table IV).

Due to the electron-accepting trifluoromethyl group at the central carbon of JA 51-DS the electrochemical reduction of this dye is facilitated. On the other hand, guanosine exhibits the most pronounced electron-donating properties among the four DNA bases.^(34–37) Considering a photoinduced electron transfer between the excited acceptor JA 51-DS and the ground-state donor guanosine, we may calculate the free energy change ΔG for this process at infinite separation:⁽³⁸⁾

$$\Delta G = E_{\text{ox}} - E_{\text{red}} - E_{0,0} \quad (2)$$

Here $E_{0,0}$ is the energy of the zero–zero transition to the lowest excited singlet state of the acceptor JA 51-DS, and E_{ox} and E_{red} are the first one-electron oxidation potential of the donor and the first one-electron reduction potential of the acceptor in the solvent under consideration. Electrochemical measurements were made for several rhodamine dyes in acetonitrile solution at a glassy carbon electrode (Table VII). For JA 51-DS we measured $E_{\text{red}} = -0.48$ V vs the saturated calomel electrode (SCE); the cyclic voltammogram indicates reversible formation of a radical anion. The first one-electron oxidation potential for deoxyguanosine $E_{\text{ox}} = 1.25$ V vs SCE in acetonitrile was taken from Ref. 36. With a zero–zero transition energy of 1.93 eV for JA 51-DS in acetonitrile we obtain a free energy change $\Delta G = -0.20$ eV for photoinduced electron transfer between the dye JA 51-DS and the DNA base guanosine in acetonitrile. Although we cannot determine the free energy change for the electron transfer in aqueous medium, because the potentials of the rhodamines cannot be measured in aqueous buffer, the trend of redox potentials of the four DNA bases in acetonitrile^(36,37) supports the occurrence of electron transfer in the case of guanosine: The free energy change for electron transfer between JA 51-DS and the four DNA bases is exergonic only for guanosine. As indicated by the reduction potentials in Table VII, this mechanism can occur more or less efficiently with all rhodamine dyes, especially with those carrying an electron-accepting group at the central carbon of the chromophore. Similar to the dimerization tendency of organic dyes, the intermolecular aggregation with the DNA nucleotides is controlled by the hydrophobicity of the dye. In case of aggregation with guanosine the resulting quenching efficiency is controlled by the redox properties of the dye. Therefore the aggregation of the dye with guanosine in aqueous buffer systems results in a complex which exhibits donor–acceptor character. In the first excited state the charge transfer interactions increase and an electron transfer from the guanosine residue to the dye occurs. Thus the fluorescence quantum

Table VII. First One-Electron Reduction Potentials E_{red} of Several Rhodamine Derivatives in Acetonitrile and Corresponding Zero–Zero Transition Energies $E_{0,0}$

Dye	E_{red} (V/SCE)	$E_{0,0}$ (eV)
JA 22	−0.71	1.96
JA 51-DS	−0.48	1.93
JA 66	−0.56	1.92
Rhodamine 6G	−0.95	2.28
Rhodamine 630	−0.82	2.16

Table VIII. Time Necessary for the Classification Between the Dyes MR200-1 and JA 51-DS Measured in Aqueous Buffer Containing 7 M Urea with an Error Rate of 10^{-4} at Different Concentrations^a

Concentration (mol/L)	6.7×10^{-10}	6.7×10^{-9}	6.7×10^{-8}	6.7×10^{-7}
Recognition time (s)	10.2	1.13	0.18	0.026

^a Measurements were done with a pulsed laser diode (636 nm, 10 μ W, 100 ps FWHM, 10 MHz repetition rate) and a PMT from a PTI spectrometer.

yield and lifetime are diminished. The short fluorescence lifetime τ_1 of the conjugates (Table IV) corresponds well to the measured times for the ground-state complexes in intermolecular experiments, whereas the longer component τ_2 represents a distribution of lifetimes resulting from free dye molecules and interactions with the other bases (mainly adenosine residues). In 7 M urea the aggregation tendency is diminished and fluorescence quenching reduced.

In spite of the above problems the two coupled dyes MR 200-1 and JA 51-DS can be distinguished by their characteristic fluorescence lifetimes using time-correlated single-photon counting technique (TCSPC). In order to reduce the number of photons, which is necessary for the identification of the dyes, data analysis based on a pattern recognition technique is used.^(15,39) This method makes use of the individual fluorescence decay patterns of the dyes, which are determined with high accuracy in separate experiments. The experimental data are compared with the reference patterns, and a classification is possible even at low signal strength. Therefore the duration of a measurement can be reduced several orders of magnitude compared to conventional lifetime determination. With the capillary setup described in the experimental section more than 10,000 photons can be collected per second. Using this technique the misclassification rate is only 8% if only 300 photons are detected.^(40,41) A mathematical technique, the so-called Cramér estimation, predicts the number of photons necessary to achieve an error rate of 10^{-4} , i.e., one mis-

classification in 10,000 experiments, to only about 1200.⁽³⁹⁾ Due to this small number, the recognition time is reduced enormously. Table VIII shows the time necessary for the classification between MR200-1 and JA 51-DS with this error rate as a function of dye concentration in 7 M urea.

CONCLUSIONS

To enhance the number of fluorescent labels in the visible–near-IR region we presented the development of new rhodamine derivatives with absorption and emission above 600 nm. Due to increasing problems with increasing absorption and emission wavelengths, such as small quantum yields and aggregation tendency in aqueous medium, we restricted our efforts to the wavelength region 620–670 nm. The new rhodamine derivatives can be excited easily with pulsed laser diodes and can be distinguished due to their characteristic fluorescence lifetime. Using the lifetime as the unequivocal characteristic, the number of fluorescent labels can be greatly enhanced. The study of the spectroscopic characteristics in aqueous environment proves the applicability of these dyes for biondiagnostics, e.g., DNA sequencing. Using different substituents, we are able to control the aggregation tendency as well as the water solubility of the dyes. Our data prove that a dye on the basis of JA 22 with a tetrachlorophenyl ring at the central carbon of the rhodamine exhibits useful fluorescence characteristics and is well suited for covalent coupling to amino groups of analytes. Additionally, this dye shows only a minimal tendency for nonspecific aggregation with biomolecules. From inter- and intramolecular experiments with DNA bases we can show that the possibility for an electron transfer between rhodamines and electron-donating molecules such as the DNA base guanosine must be taken into consideration. This process reduces the fluorescence quantum yield. In view of to new DNA-sequencing methods based on single fluorescent label detection,^(42–45) the behavior mentioned above is of great importance. In order to prevent an interaction between such dyes and the DNA bases, other coupling positions as well as other spacer lengths have to be investigated. We are in the process of developing new nonsymmetric rhodamines based on the dye JA 22. Here one of the amino groups is connected with a linker and a carboxyl group for covalent coupling, whereas to the other amino group an electron-donating or -accepting substituent is attached which controls the lifetime of the excited state without changing the other spectroscopic characteristics. These

dyes will be excitable by a single diode laser and identified by the differences in fluorescence lifetime.

ACKNOWLEDGMENTS

We would like to thank Photon Technology International for generously making available the LS 100 spectrometer and the Bundesministerium für Forschung und Technologie for financial support under grants 0310183 A and 0310158 A. The financial support of the Deutsche Forschungsgemeinschaft and of the Fond der Chemischen Industrie are also gratefully acknowledged.

REFERENCES

1. L. M. Smith, S. Fung, M. W. Hunkapillar, and L. E. Hood (1985) *Nucleic Acids Res.* **13**, 2399.
2. W. Ansorge, B. Sproat, J. Stegemann, J. Erfle, and H. Voss Nucl. (1990) *Nucleic Acids Res.* **18**, 3419.
3. J. M. Prober, G. L. Trainer, R. J. Dam, F. W. Hobbs, C. W. Robertson, R. J. Zagursky, A. J. Cocuzza, M. A. Jensen, and K. Baumeister (1987) *Science* **238**, 336.
4. R. S. Davidson and M. M. Hilchenbach (1990) *Photochem. Photobiol.* **52**, 431.
5. I. A. Hemmilä (1989) *Appl. Fluoresc. Technol.* **1**, 1.
6. H. Coons, H. J. Creech, R. N. Jones, and E. Berliner (1942) *J. Immunol. Meth.* **45**, 159.
7. J. L. Riggs, R. J. Seidwald, J. H. Burckhalter, C. M. Downs, and T. G. Metcalf (1958) *Am. J. Pathol.* **34**, 1081.
8. K. H. Drexhage (1973) in F. P. Schäfer (Ed.), *Dye Lasers* Springer-Verlag, Berlin, Chapter 4.
9. J. Arden, G. Deltau, V. Huth, U. Kringel, D. Peros, and K. H. Drexhage (1991) *J. Luminesc.* **48&49**, 352.
10. M. Sauer, J. Arden-Jacob, G. Deltau, K. H. Drexhage, A. Schulz, S. Seeger, and J. Wolfrum (1993) *Ber. Bunsenges. Phys. Chem.* **97**, 1734.
11. M. Sauer, K.-T. Han, R. Müller, A. Schulz, R. Tadday, S. Seeger, J. Wolfrum, J. Arden-Jacob, G. Deltau, N. J. Marx, and K. H. Drexhage (1993) *J. Fluoresc.* **3**, 131.
12. M. Sauer, J. Arden-Jacob, V. Ebert, G. Deltau, K. H. Drexhage, K.-T. Han, N. J. Marx, R. Müller, S. Seeger, A. Schulz, and J. Wolfrum (1994) in *Proceedings SPIE Time-Resolved Laser Spectroscopy in Biochemistry IV* (1994), pp. 762–773.
13. G. Bachteler, J. Arden-Jacob, K. H. Drexhage, K.-T. Han, M. Köllner, R. Müller, M. Sauer, S. Seeger, and J. Wolfrum (1994) *J. Luminesc.* **60&61**, 511.
14. S. Seeger, G. Bachteler, J. Arden-Jacob, G. Deltau, K. H. Drexhage, K.-T. Han, M. Köllner, R. Müller, M. Sauer, A. Schulz, and J. Wolfrum (1993) *Ber. Bunsenges Phys. Chem.* **97**, 1542.
15. M. Köllner (1993) *Appl. Opt.* **32**, 806.
16. J. Arden-Jacob (1992) Ph.D. Thesis, Siegen.
17. German Patent DE 4137934 (17.11.1992).
18. A. V. Azhayev, A. M. Ozols, A. S. Bushnev, N. B. Dyatkina, S. V. Kochetkova, L. S. Victorova, M. K. Kukhanova, A. A. Krayevsky, and B. P. Gottikh (1979) *Nucleic Acids Res.* **6**, 625.
19. K.-T. Han, M. Sauer, A. Schulz, S. Seeger, and J. Wolfrum (1993) *Ber. Bunsenges. Phys. Chem.* **97**, 1728.
20. W. Bannwarth and R. Knorr (1990) *Helv. Chim. Acta* **1990**, 1157–1160.
21. R. R. Alfano, S. L. Shapiro, and W. Yu (1973) *Opt. Commun.* **7**, 191.

22. C. Zander (1991) Ph.D. Thesis, Siegen.
23. A. E. Boyer, M. Lipowska, J.-M. Zen, G. Patonay, and V. C. W. Tsung (1992) *Anal. Lett.* **25**, 415.
24. P. L. Southwick, L. A. Ernst, E. V. Tauriello, S. R. Parker, R. B. Mujumdar, S. R. Mujumdar, H. A. Clever, and A. S. Waggoner (1990) *Cytometry* **11**, 418.
25. R. B. Mujumdar, L. A. Ernst, S. R. Mujumdar, and A. S. Waggoner (1989) *Cytometry* **10**, 11.
26. E. Terpetschnig, H. Szmanski, A. Ozinskas, and J. R. Lakowicz (1994) *Anal. Biochem.* **217**, 197.
27. H. Kuhn (1959) in D. L. Zechmeister (Ed.), *Progress in the Chemistry of Organic Natural Products, Vol. 16*, Springer-Verlag, Berlin.
28. V. K. Kelkar, B. S. Valaulikar, J. T. Kunjappu, and C. Manohar (1990) *Photochem. Photobiol.* **52**, 717.
29. V. I. Yuzhakov (1979) *Russ. Chem. Rev.* **48**, 1076.
30. V. I. Yuzhakov (1992) *Russ. Chem. Rev.* **61**, 613.
31. J. E. Selwyn and J. I. Steinfeld (1972) *J. Phys. Chem.* **76**, 762.
32. F. Sanger, S. Nicklen, and A. R. Coulson (1977) *Proc. Natl. Acad. Sci. USA* **74**, 5463.
33. K.-T. Han, M. Sauer, K. H. Drexhage, and J. Wolfrum (1994) in preparation.
34. D. Nikogosyan (1990) *Int. J. Radiat. Biol.* **57**(2), 233.
35. L. Kittler, G. Löber, F. Gollmick, and H. Berg (1980) *J. Electroanal. Chem.* **116**, 503.
36. C. Seidel, A. Schulz, and M. Sauer (1994) *J. Phys. Chem.* (submitted).
37. C. Seidel (1992) Ph. D. Thesis, Heidelberg.
38. D. Rehm and A. Weller (1970) *Isr. J. Chem.* **8**, 259.
39. M. Köllner and J. Wolfrum (1992) *Chem. Phys. Lett.* **200**, 199.
40. S. Seeger, J. Arden-Jacob, N. Marx, K.-H. Drexhage, K. Galla, M. Martin, K.-T. Han, M. Köllner, R. Müller, M. Sauer, and J. Wolfrum (1994) *Proc. SPIE* **2136**, 75.
41. R. Müller, G. Bachteler, K. T. Han, M. Sauer, S. Seeger, J. Wolfrum, J. Arden-Jacob, N. J. Marx, K. H. Drexhage (1994) Ultra-sensitive detection of biomolecules with multiplex dyes and diode lasers in capillary gel electrophoresis, in *Würzburger Kolloquium, Kapillarelektrophorese, Chromatographie*, Bertsch Verlag, pp. 87-95.
42. J. H. Jett, R. A. Keller, J. C. Martin, B. L. Marrone, R. K. Moyzis, R. L. Ratliff, N. K. Seitzinger, E. B. Shera, and C. C. Stewart (1989) *J. Biomol. Struct. Dynam.* **7**, 301.
43. S. A. Soper, L. M. Davis, F. R. Fairfield, M. L. Hammond, C. A. Harger, J. H. Jett, R. A. Keller, B. L. Marrone, J. C. Martin, H. L. Nutter, E. B. Shera, and D. J. Simpson (1991) *Proc. Int. Soc. Opt. Eng.* **1435**, 168.
44. S. A. Soper, L. M. Davis, and E. B. Shera (1992) *J. Opt. Soc. Am. B* **9**(10), 1761.
45. W. Ambrose, P. M. Goodwin, J. H. Jett, M. E. Johnson, J. C. Martin, B. L. Marrone, J. A. Schecker, C. W. Wilkerson, R. A. Keller, A. Haces, P.-J. Shih, and J. D. Harding (1993) *Ber. Bunsenges. Phys. Chem.* **97**, 1535.